Estimation of Material Parameters in Nonlinear Hardening Plasticity Models and Strain Life Curves for CuAg Alloy

Estimation of Material Parameters in Nonlinear Hardening Plasticity Models and Strain Life Curves for CuAg Alloy

J Srnec Novak[1], D Benasciutti[1], F De Bona[1], A Stanojević[2], A De Luca[3], Y Raffaglio[3]

[1]DIEGM, University of Udine, Via delle Scienze 206, Udine 33100, Italy
[2]Chair of Mechanical Engineering, Montanuniversität Leoben, Franz Josef-Straße 18, Leoben 8700, Austria
[3]Centro Ricerche Danieli, Via Nazionale 41, Buttrio (UD) 33042, Italy

E-mail: jelena.srnec@uniud.it

Abstract. This work investigates the cyclic response and low-cycle fatigue behaviour of a CuAg alloy used in crystallizer for continuous casting lines. Therefore isothermal strain-based fatigue tests are first performed on CuAg specimens at different temperature levels (20 °C, 250 °C, 300 °C). The evolution of stress-strain loops recorded during the cyclic tests is used for the parameter identification of several nonlinear hardening models (nonlinear kinematic, nonlinear isotropic). Cyclic stress-strain data from experiments are compared with results from numerical simulations with the identified material parameters, showing a satisfying agreement. Critical examination of numerical results from different models is also performed. Finally, the strain-life fatigue curves estimated from experimental data are compared with approximate strain-life equations (Universal Slopes Equation, 10% Rule) which are obtained from simple tensile tests. The material parameters determined in this work can conveniently be used as inputs in a elasto-plastic finite element simulations of a crystallizer.

1. Introduction

Mechanical components in steel-making plants are often exposed to cyclic thermo-mechanical loadings and then exhibit a cyclic elasto-plastic behaviour and fatigue damage. In continuous casting lines, a typical example is the crystallizer, which is a long hollow component where the molten steel starts to solidify. Thermo-mechanical finite element (FE) analysis requires suitable models to properly simulate the cyclic elasto-plastic material response of the crystallizer as well as other components under thermo-mechanical loading (e.g. anode of electric arc furnace). The cyclic stresses and strains calculated by FE simulations are then compared to the experimentally obtained fatigue lives in order to estimate the component service life.

Over the last fifty years several theories to describe the elasto-plastic and viscoplastic material behaviour (plasticity, creep, relaxation) have been developed and further improved [1-3]. Some of them have become readily available in commercial finite element software and are used for every-day industrial design.

The capability of a material model to correctly represent a material behaviour observed in experiments is the first criterion for model selection. Material models generally depend on several parameters, which have to be calibrated on experimental results. By increasing the model complexity the number

of material parameters usually increases as well. Complex numerical algorithms are often used to identify multiple parameters simultaneously and optimisation routines are recommended [4-6].
Sometimes it may be difficult, especially for non-experienced engineers, to understand which model is most suitable for their application or which parameters do really affect the material response. The choice of the material model for FE simulations, especially in industrial applications, often is the result of a trade-off among various needs, such as model complexity, computation time and experimental data available for parameter identification.
As a contribution to material modelling and parameter identification this work presents the results of a research activity aimed at experimental testing and parameter identification of a CuAg alloy used for crystallizers of continuous casting lines. Isothermal strain-based low-cycle fatigue (LCF) tests are performed at different temperatures (20 °C, 250 °C, 300 °C). Experimental stress-strain loops are used for parameter identification of nonlinear kinematic (Armstrong-Frederick, Chaboche) and nonlinear isotropic hardening models. Numerical simulations with the identified material parameters are then compared with experimental data, showing that the considered material models are adequate to represent the elasto-plastic behaviour of the CuAg alloy. Strain-life fatigue lines estimated from experimental data are finally compared with some approximate analytical equations (Universal Slopes Equation, 10% Rule), which are estimated from simple tensile tests.

2. Nonlinear hardening models: theoretical background

The combined material model (nonlinear kinematic + nonlinear isotropic) is able to capture elasto-plastic behaviour of a material under cyclic loading. In the case of combined hardening, the yield surface can both translate and expand as shown in Figure 1. The von Mises yield criterion is given by:

$$f = \sqrt{\frac{3}{2}\left(\boldsymbol{\sigma}'-\boldsymbol{\alpha}'\right):\left(\boldsymbol{\sigma}'-\boldsymbol{\alpha}'\right)} - R - \sigma_0 = 0 \tag{1}$$

where $\boldsymbol{\sigma}'$ and $\boldsymbol{\alpha}'$ are the deviatoric parts of the stress and the back stress tensor, respectively, σ_0 is the initial yield stress and R is the drag stress. Kinematic part is controlled by $\boldsymbol{\alpha}$ (translation of the yield surface), while the isotropic part is related to R (expansion of the yield surface). The simplest kinematic model is the linear kinematic hardening model developed by Prager (1949), which assumes that the evolution of $\boldsymbol{\alpha}$ is collinear with the plastic strain tensor:

$$\mathrm{d}\boldsymbol{\alpha} = \frac{2}{3} C \mathrm{d}\boldsymbol{\varepsilon}_{\mathrm{pl}} \tag{2}$$

where C is the initial hardening modulus. Armstrong and Frederick (1966) modified Prager's model by adding a recall term, which introduces a fading memory effect to the strain path. The recall term is called dynamic recovery. As a result, the nonlinear evolution of $\boldsymbol{\alpha}$ is obtained [1]:

$$\mathrm{d}\boldsymbol{\alpha} = \frac{2}{3} C \mathrm{d}\boldsymbol{\varepsilon}_{\mathrm{pl}} - \gamma \boldsymbol{\alpha} \mathrm{d}\varepsilon_{\mathrm{pl,acc}} \tag{3}$$

where γ defines the rate at which hardening modulus starts to decrease as the plastic strain develops. Chaboche further extended the Armstrong-Frederick model by superimposing two or more nonlinear kinematic hardening models:

$$\boldsymbol{\alpha} = \sum_i \boldsymbol{\alpha}_i \quad ; \quad \mathrm{d}\boldsymbol{\alpha}_i = \frac{2}{3} C_i \mathrm{d}\boldsymbol{\varepsilon}_{\mathrm{pl}} - \gamma_i \boldsymbol{\alpha}_i \mathrm{d}\varepsilon_{\mathrm{pl,acc}} \tag{4}$$

The integration of equation (3) with respect to $\varepsilon_{\mathrm{pl}}$, for uniaxial loading, leads to:

$$\alpha = \psi \frac{C}{\gamma} + \left(\alpha_0 - \psi \frac{C}{\gamma} \right) \exp\left[-\psi\gamma\left(\varepsilon_{\mathrm{pl}} - \varepsilon_{\mathrm{pl},0} \right) \right] \tag{5}$$

where ψ=±1 indicates the flow direction, $\varepsilon_{\mathrm{pl},0}$ and α_0 are the initial values of plastic strain and back stress, respectively, at the beginning of the considered loading branch. Assuming tension (ψ=1) and zero initial plastic strain and back stress, equation (5) becomes:

$$\sigma = \sigma_0 + \frac{C}{\gamma}\left[1 - \exp\left(-\gamma\varepsilon_{\mathrm{pl}} \right) \right] \tag{6}$$

Equation (6) is proposed to estimate material parameters C and γ from a single stabilized stress-strain loop [1, 7]. Analytical integration of (5), for tension and compression, gives the relation between the stress amplitude and the plastic strain amplitude for the stabilized cycle [1, 7]:

$$\sigma_{\mathrm{a}} = \sigma_0 + \frac{C}{\gamma} \tanh\left(\gamma\varepsilon_{\mathrm{pl,a}} \right) \tag{7}$$

or in the form of Chaboche model:

$$\sigma_{\mathrm{a}} = \sigma_0 + \sum_{i=1} \frac{C_i}{\gamma_i} \tanh\left(\gamma_i\varepsilon_{\mathrm{pl,a}} \right) \tag{8}$$

where σ_{a} is the stress amplitude and $\varepsilon_{\mathrm{pl,a}}$ is the plastic strain amplitude. Equation (7) and (8) are suitable to estimate parameters from several stabilized stress-strain curves [1].

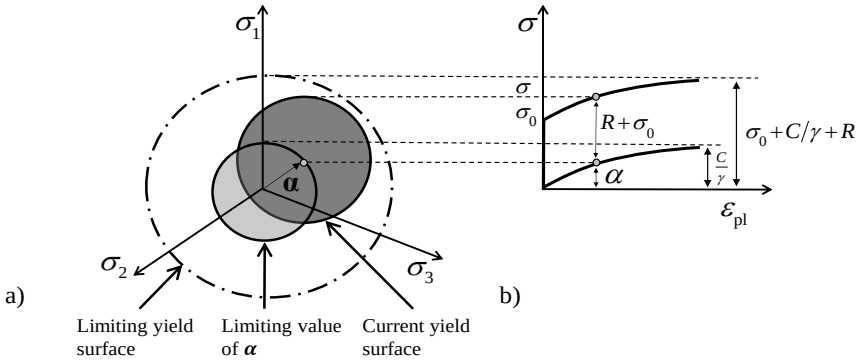

Figure 1. Schematic evolution of the combined hardening model: a) in stress space and b) in uniaxial tension.

The nonlinear isotropic hardening is expressed by the following equation [1]:

$$\mathrm{d}R = b\left(R_\infty - R \right) \mathrm{d}\varepsilon_{\mathrm{pl,acc}} \tag{9}$$

where R_∞ is the saturation value of the yield surface, b is the speed of stabilization and $\varepsilon_{\mathrm{pl,acc}}$ is the accumulated plastic strain. R_∞ can be either positive or negative, giving rise to cyclic hardening or softening, respectively. The relation between R and $\varepsilon_{\mathrm{pl,acc}}$ is obtained after integration:

$$R = R_\infty \left[1 - \exp\left(-b\varepsilon_{\mathrm{pl,acc}} \right) \right] \tag{10}$$

3. Experimental testing

Isothermal low cycle fatigue (LCF) tests were performed to characterize the cyclic stress-strain behaviour and fatigue life of CuAg alloy at three temperature levels (20 °C, 250 °C, 300 °C). Several specimens were tested at different strain ranges for each temperature. All isothermal LCF tests were carried out in strain controlled mode with a triangular loading waveform and with a fully reversed strain ratio R_ε=-1. The examined strain rate was 0.01 s^{-1}. Tests were interrupted before specimen failure when the maximal stress decreased by 80%. LCF testing at 20 °C were performed on the servo-hydraulic Instron-Schenck test rig with a nominal force ±250 kN, while the Instron extensometer with a gauge length of 12.5 mm and a range of ±5 mm was used to measure elongation during testing. The specimens were clamped by mechanical clamping grips. LCF testing at 250 °C and 300 °C were performed on the Instron test rig with a nominal force of ±100 kN. The temperature was applied by the induction heating system with a 10 kW medium frequency generator, Hüttinger TIG 10/300. The temperature was measured within the gauge length with a pre-stressed type K loop thermocouple. To measure an elongation at high temperatures an MTS extensometer, model 632.53F-14 with a gauge length of 12.6 mm and a range of ±1.8 mm was used. Test specimens were clamped by water cooled hydraulic clamping grips. Results of experimental tests are used for model calibration and estimation of the strain-life equations, as shown in the next paragraphs.

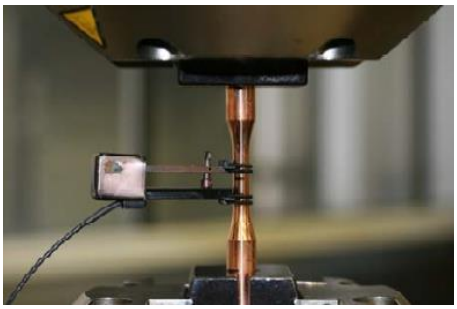

Figure 2. Mechanical clamping jaws with extensometer for room temperature.

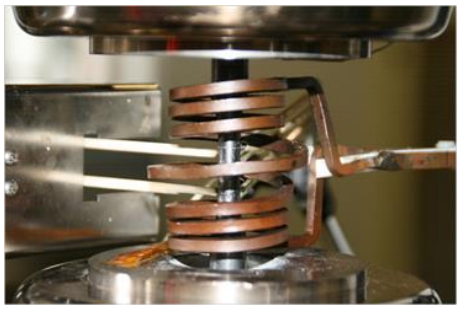

Figure 3. Hydraulic clamping jaws, HT extensometer and heating apparatus.

4. Identification of material parameters

Firstly, the Young's modulus and the yield stress were estimated as they define the elastic region. The Young's modulus was determined by using both the tensile portion of the first hysteresis loop (E_1) and the stabilized stress-strain loop (E_s). As shown in Table 1, the Young's modulus is a function of the temperature and it also seems to depend on the applied strain amplitude (ε_a). Furthermore, the Young's modulus seems to slightly decrease during the applied cyclic loading.

Table 1. Estimated values of the Young's modulus.

Temp. (°C)	ε_a=0.3%		ε_a=0.4%		ε_a=0.5%		ε_a=0.7%		Average values	
	E_1 (MPa)	E_s (MPa)	E_1 (MPa)	E_s (MPa)	E_1 (MPa)	E_s (MPa)	E_1 (MPa)	E_s (MPa)	E_1 (MPa)	E_s (MPa)
20	119700	116900	119900	115900	118200	113500	118800	114900	119080	110900
250	108500	93760	108600[a]	98530[a]	105400	90140	103900	85100	106600	94758
300	105600	97930	104300	98820	101900	95770	103400	87690	103800	94792

[a] ε_a=0.35%

The initial yield stress (σ_0) was identified as a point on the tensile portion of the first hysteresis loop where plastic strain occurs; the actual yield stress (σ_{0*}) was measured by using the stabilized stress-strain loop (at half number of cycles to failure). The evolution of the yield stress with increasing

number of cycles enabled to determine the hardening or softening characteristics of the material, as can be seen in Table 2. In all evaluated cases $\sigma_{0*} < \sigma_0$, confirming a softening behaviour of the material.

Table 2. Estimated values of the yield stress.

Temp. (°C)	ε_a=0.3%		ε_a=0.4%		ε_a=0.5%		ε_a=0.7%		Average values	
	σ_0 (MPa)	σ_{0*} (MPa)	σ_0 (MPa)	σ_{0*} (MPa)	σ_0 (MPa)	σ_{0*} (MPa)	σ_0 (MPa)	σ_{0*} (MPa)	σ_0 (MPa)	σ_{0*} (MPa)
20	121.64	87.95	138.76	91.44	117.97	84.25	154.94	114	130	86
250	111.34[a]	51.71[a]	103.46	50.86	140.31	50.98	80.68	53.47	113	50
300	124	44.7	103.3	48.23	116.37	40.49	122.5	43.48	110	45

[a] ε_a=0.35%

The estimation procedure of nonlinear kinematic parameters (C_i, γ_i) and nonlinear isotropic parameters (R_∞, b) could be performed separately. In fact, for fully-reversed symmetrical stress cycles the kinematic model stabilizes after a single cycle. As the contribution of the isotropic model in the first cycle is actually small, it could be neglected [1]. Similarly the kinematic model does not influence significantly the subsequent cycles.

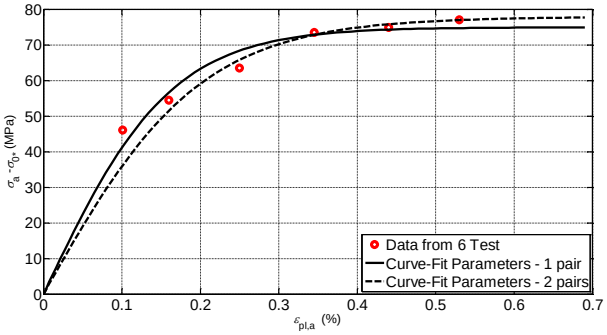

Figure 4. Curve fitting by the least squares method, using data of 6 hysteresis loops (T=20 °C).

Nonlinear kinematic hardening material parameters, C_i and γ_i were estimated after the determination of Young's modulus and yield stress. One and two pairs of material parameters were estimated using only the plastic regions of each stabilized cycle obtained under imposed ε_a. For a given stress-strain loop, the stress amplitude (σ_a), the plastic strain amplitude ($\varepsilon_{pl,a}$) and the actual yield stress (σ_{0*}) were measured at a stabilized cycle (half-life cycle) and plotted as in Figure 4. The procedure was repeated at each strain amplitude. Equations (7) and (8) were fitted to the measured points to obtain one and two pairs of material parameters C_i, γ_i, respectively. The material parameters obtained by the method here described are suitable to be used for different ε_a values.

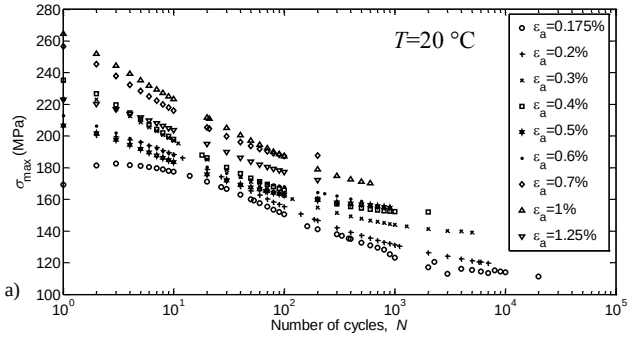

Figure 5. Stress amplitude vs. number of cycles.

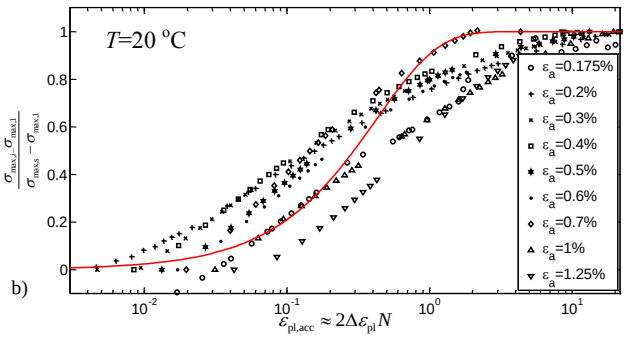

Figure 6. Fitting of Eq. (13) to find parameter b.

Nonlinear isotropic parameters were finally estimated. The maximum stress (σ_{max}) was measured for each stress-strain cycle and plotted against the number of applied cycles (N), see Figure 5, showing a softening behaviour. The procedure was repeated for each imposed strain amplitude and temperature. The saturation stress (R_∞) was determined as the difference in the maximum stress of the first cycle ($\sigma_{max,1}$) and the stabilized one ($\sigma_{max,s}$). Figure 5 shows that the saturation stress (R_∞) depends also on the applied strain amplitude; this behaviour was also observed in [4] for a nickel base superalloy. For each temperature an average R_∞ is calculated, see Table 3. The speed of stabilization (b) is estimated by fitting to experimental data (see Figure 6) the following expression proposed by [1]:

$$\frac{\sigma_{max,i}-\sigma_{max,1}}{\sigma_{max,s}-\sigma_{max,1}} \cong \frac{R}{R_\infty} = 1-\exp\left(-b\varepsilon_{pl,acc}\right) = 1-\exp\left(-2b\Delta\varepsilon_{pl}N\right) \quad (11)$$

where $\sigma_{max,i}$ is the current maximum stress for the N^{th} cycle. Equation (11) is shown in Figure 6. A reasonable correlation is obtained, although a modification of the evolution rule of R seems necessary. Estimated material parameters used in numerical simulations are shown in Table 3.

Table 3. Estimated material parameters used in numerical simulations.

					One pair		Two pairs			
Temp. (°C)	E (MPa)	σ_0 (MPa)	R_∞ (MPa)	b	C_1 (MPa)	γ_1	C_1 (MPa)	γ_1	C_2 (MPa)	γ_2
20	119080	130	-75.7	2.352	46250	617.2	38160	505.7	679.5	274
250	106600	113	-80.2	3.894	45340	820.9	290600	8699	8772	349.5
300	103800	110	-76.6	5.293	40080	832.8	27530	894.9	12760	731.1

5. Numerical simulation

Figure 7 a)-c) shows a comparison between experimental data and results of numerical simulations for a uniaxial cyclic loading. Simulations are performed with the material parameters identified in the previous Section. The nonlinear kinematic model uses both one and two pairs of (C_i, γ_i) parameters, estimated at 20 °C, 250 °C and 300 °C. A better agreement between experimental and simulated data is obtained with only one pair of parameter at 20 °C, 250 °C; while at 300 °C one and two pairs give quite the same shape of stress-stain loops.

The comparison between experimental and simulated stress-strain loops is also performed at different strain amplitudes (ε_a) to confirm that the estimated material parameters are suitable to be used over a wider interval of strain ranges. As can be seen in Figure 8, all three simulations are in good accordance with the experimental data. Based on the obtained results, a kinematic model with only one pair is used in the following simulations.

Finally, the combined kinematic and isotropic material model is used to simulate 50 cycles at strain amplitude ε_a=0.5%. Material parameters used in the simulation are taken from Table 3. Comparison between experimental stress-strain loops (1st and stabilized cycle) and simulated loops (every 5th cycle is plotted for a better overview) is shown in Figure 9. It has to be noted, however, that the small value of b does not allow the material to reach the stabilized state within the simulated 50 cycles.

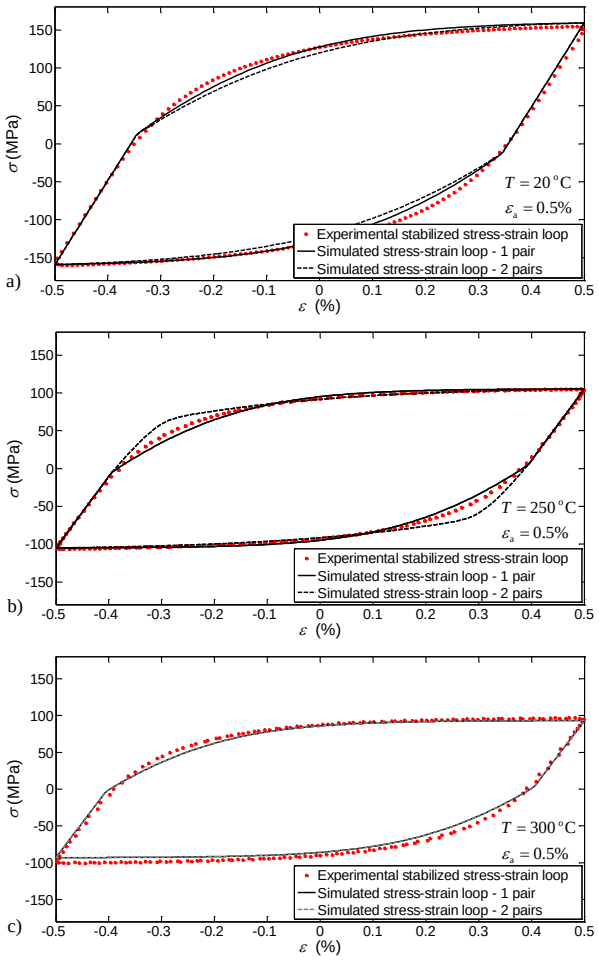

Figure 7. Comparison between experimental and simulated stress-strain loops obtained with one and two (C_i, γ_i) pairs at different temperatures.

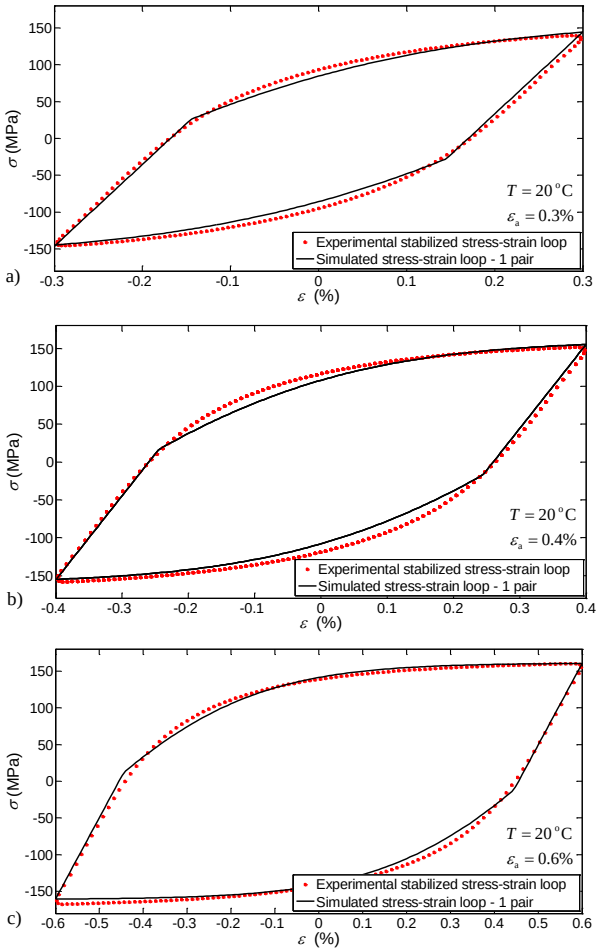

Figure 8. Comparison between experimental and simulated stress-strain loops for different values of ε_a.

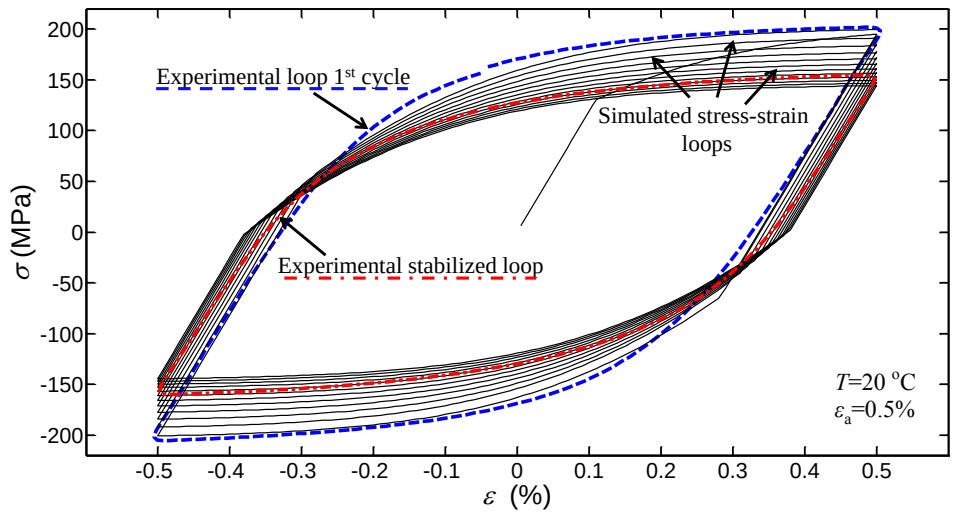

Figure 9. Comparison between experimental and simulated stress strain loops for combined material model.

6. Strain-life fatigue curves

The Manson–Coffin-Basquin equation is used to relate the cycles to failure N_f to the strain amplitude [8]:

$$\frac{\Delta\varepsilon}{2} = \frac{\Delta\varepsilon_{el}}{2} + \frac{\Delta\varepsilon_{pl}}{2} = \frac{\sigma'_f}{E}(2N_f)^e + \varepsilon'_f(2N_f)^c \quad (12)$$

where $\Delta\varepsilon$, $\Delta\varepsilon_{el}$, $\Delta\varepsilon_{pl}$ are total, elastic and plastic strain ranges, respectively. The fatigue strength coefficient (σ'_f), fatigue strength exponent (e), fatigue ductility coefficient (ε'_f) and fatigue ductility exponent (c) are estimated from isothermal LCF data at different temperature, see Table 4.

Table 4. Estimated material parameters used in numerical simulations.

Temp. (°C)	σ'_f (MPa)	e	ε'_f	c
20	359.1	-0.1031	0.07689	-0.3942
250	253.6	-0.1018	0.2942	-0.5311
300	240.4	-0.1068	0.4258	-0.5708

Approximate methods are often used to estimate the strain-life curve from static strength data. An example is the Universal Slopes (US) equation, which assumes that, for all materials, elastic and plastic lines have unique slopes 0.12 and 0.6, respectively:

$$\Delta\varepsilon = \Delta\varepsilon_{el} + \Delta\varepsilon_{pl} = 3.5\frac{\sigma_{uts}}{E}N_f^{-0.12} + D^{0.6}N_f^{-0.6} \quad (13)$$

where σ_{uts} is the ultimate tensile strength and D is the ductility, which is related to the cross-area reduction in a tensile test. Although the US equation was originally proposed for steel at room temperature [9], an attempt is made here to apply it to CuAg alloy at 20 °C and 250 °C.

Influence of high temperatures and creep can reduce fatigue life by up to 90%. Therefore, 10% Rule assumes that at high temperature, only 10% of the life estimated by the US equation will actually be achieved. The upper bound of time life is then given by the US equation, while the lower bound of time life is given by the 10% Rule.

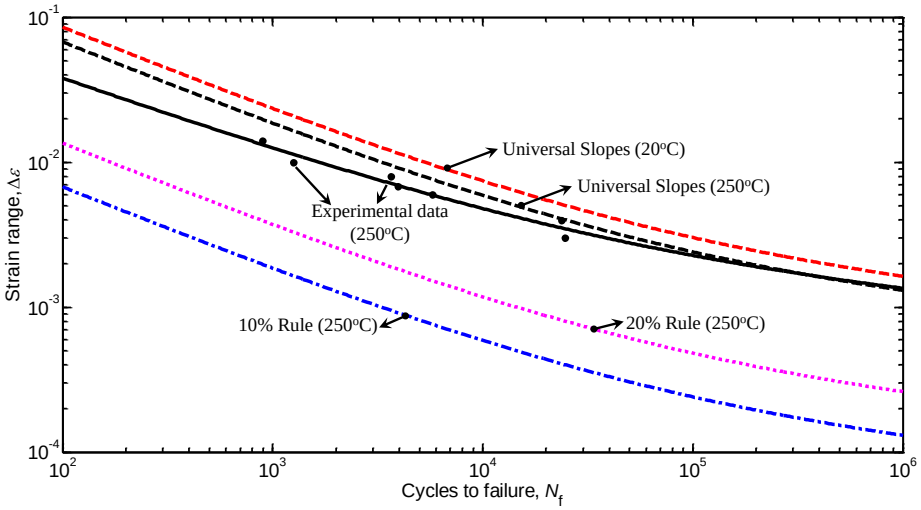

Figure 10. Comparison of strain-life curves.

Figure 10 shows a comparison of strain-life curves, estimated by different methods. The US equation (20 °C - upper bound) seems to be under conservative compared to the US (250 °C) curve. Therefore, to be on a safe side, the 10 % Rule (lower bound) and the 20% Rule (average) were calculated based

on US (250 ^{o}C). It is worth noting how the 10% Rule seems to be over conservative, at least for this alloy at this temperature.

7. Conclusions

This work investigates the cyclic response and the fatigue life of a CuAg alloy. Isothermal low-cycle fatigue tests have been performed at different temperatures (20 ^{o}C, 250 °C, 300 °C) to determine the stress-strain response and the experimental fatigue life. Several material models (nonlinear kinematic, nonlinear isotropic) have been then calibrated with experimental results. In particular, parameters for the nonlinear kinematic model (one and two pairs of C_i, γ_i) have been estimated from LCF experimental data, as well as parameters for nonlinear isotropic model (R_∞, b). Numerical simulations for uniaxial loading with the identified material parameters have been compared with experimental results, showing a quite good agreement. Finally, the strain-life curves estimated from experimental data have been also compared with approximate methods (Universal Slopes Equation, 10% Rule), which estimate the strain-life curve from static strength data of a tensile test. A satisfactory agreement has been observed.

The results presented in this work would thus permit/allow one to perform an effective service life assessment of steel-making components made of CuAg alloy, when a design approach based on Finite Element modelling and elasto-plastic analysis have to be followed.

References

[1] Lemaitre J and Chaboche J L 1990 *Mechanic of Solid Materials* (Cambridge: Cambridge University Press)
[2] Chaboche J L 2008 A review of some plasticity and viscoplasticity constitutive theories *Int. J. Plasticity* **24** 1642–1693
[3] Chaboche J L and Rousselier G 1983 On the plastic and viscoplastic constitutive equations – Part I: Rules developed with internal variable concept *J. of Pressure Vessel Technol.* **105** 153-158
[4] Zhao L G, Tong B, Vermeulen B and Byrne J 2001 On the uniaxial mechanical behaviour of an advanced nickel base superalloy at high temperature *Mech. Mater.* **33** 593-600
[5] Broggiato G B, Campana F and Cortese L 2008 The Chaboche nonlinear kinematic hardening model: calibration methodology and validation *Meccanica* **43** 115–124
[6] Franulovic M, Basan R and Prebil I 2009 Genetic algorithm in material model parameters' identification for low-cycle fatigue *Comput. Mater. Sci.* **45** 505–510
[7] Halama R, Sedlak J and Šofer M 2012 Phenomenological modelling of cyclic plasticity Numerical Modelling edited by Peep Miidla *Intech* 329-351
[8] Manson S S and Halford G R 2006 *Fatigue and Durability of Structural Materials* ASM International
[9] Manson S S 1968 A simple procedure for estimating high-temperature low-cycle fatigue, *Exp. Mechanics* **8** 349-355